Development of Textured Antireflective Layers for Optical Path Length Enhancement in Solar Cells

Thesis

Presented in Partial Fulfillment of the Requirements for Undergraduate Research Distinction in the College of Engineering at The Ohio State University

By

Allison C. Whitney

With distinction in Materials Science and Engineering

The Ohio State University

2020

Thesis Committee

Tyler J. Grassman, Advisor

Heather Powell, Committee Member

Abstract

This research examined various methods of developing a permanent antireflective coating (ARC) for III-V type solar cells using non-destructive methods. It was determined that polydimethylsiloxane (PDMS) could be successfully used as a transfer medium from three different sources. The three textures examined were random texture from polishing paper, biomimetic texture from a rose petal, and pyramidal pattern texture transferred from a textured silicon wafer. These textures were examined to determine the efficacy of PDMS as an imprint material. The pyramidal textured sheet was examined to see how it affected light scattering tested via a light scan and greyscale image analysis, and how it affected device efficiency via solar simulator testing on a III-V solar device. An increase in short circuit current was observed when the textured PDMS was applied to the device. Significant light scattering was also seen and quantified by fitting an averaged light scan to a pseudo-Voigt model via MATLAB light scan analysis as a 74.2% increase in the full width half max light profile with addition of a textured PDMS sheet. Due to the limited lifespan of PDMS as an ARC, the sol-gel method was tested as a permanent thin film ARC on III-V type devices. The texture transfer process was tested using a silica sol-gel solution and formed a thin film; however, more testing is required to determine the viability of developing a textured sol-gel thin film for solar cells.

Acknowledgments

This research would not have been possible without the help of the Electronic Materials and Devices group under the divine guidance of Tyler Grassman, including Daniel Lepkowski, Zak Blumer, Ari Blumer, and Jacob Boyer.

Vita

Education

The Ohio State University (Columbus, Ohio): 2016-2020

Work Experience

Metzenbaum Sheltered Industries (Chesterland, Ohio): Summer 2017

The Institute of Aviation (Warsaw, Poland): Summer 2018

GE Aviation (Cincinnati, Ohio): Summer 2019

GE Healthcare (Milwaukee, Wisconsin): Post-graduation

Field of Study

Major Field: B.S., Materials Science and Engineering

Table of Contents

Abstract iii
Acknowledgments iv
Vita v
List of Figures viii
Chapter 1. Introduction 1
1.1 Antireflective coatings and textures 1
1.1.1 Pyramidal texture 2
1.1.2 Random texture 2
1.1.3 Biomimetic texture 3
1.2 Polydimethylsiloxane texturization 3
1.3 Sol-gel 4
1.4 Objective Statement 5
Chapter 2. Methodology 6
2.1 Textured polydimethylsiloxane fabrication 6
2.1.1 PDMS light scan testing 7
2.1.2 PDMS gray scale image testing 8
2.1.3 PDMS solar simulating testing 8
2.2 Sol-gel synthesis and testing 8
2.2.1 Sol-gel evaporation testing 9
2.2.2 Sol-gel thin film testing 9
2.2.3 Rapid evaporation 10
Chapter 3: PDMS Texturization 12
3.1 Random Texturization 12
3.1.1 Profilometry 13
3.2 Biomimetic 14

Chapter 4: PDMS Optical Characterization and Testing 15
4.1 Light Scan Analysis 15
4.2 Grayscale Image Light Scatter Testing 15
4.3 Solar Simulator Analysis 16
Chapter 5: Sol Gel Fabrication and Analysis 18
5.1 Sol gel evaporation testing 18
5.2 Sol-gel wafer drop coat application 19
5.3 Sol gel wafer spin coat application 20
5.4 Sol gel rapid heating 21
Chapter 6: Conclusion 23
6.1 PDMS 23
6.1.1 PDMS texturization 23
6.1.2 PDMS optical analysis 23
6.2 Sol gel 23
6.3 Future work 23
Bibliography 25

List of Figures

Figure 1: Increase in current density with addition of an antireflective coating [Marko] .. 2
Figure 2: Reflection of incident light from (a) Bare planar Si and (b) Si micro pyramid texture [Al-Husseini] 2
Figure 3: Cross section representation of a replicated rose structure coating on a substrate showing the light focusing effect. Adapted from [Hunig] 3
Figure 4: Simulated reflectance for 40 µm Si substrate with a 4 µm thick textured PDMS film on top. Adapted from [Rosell] 4
Figure 5: White-light interferometry measurement to of SiO_2 layer surface to determine area roughness [Thor] 5
Figure 6: Textured PDMS sheet process schematic 6
Figure 7: Processing of rose petal textured PDMS sheet (a) prior to petal removal and solvent sonification and (b) after solvent sonification and prior to final rinse 7
Figure 8: Light scan testing set-up 8
Figure 9: Flow chart of silica sol-gel processing 9
Figure 10: Drop coat (a) applied to a silicon wafer and (b) after being covered 10
Figure 11: 50x magnification image of PDMS textured with polishing paper 12
Figure 12: 6 µm polishing paper (top) and PDMS textured with the 6 µm paper (bottom) 13
Figure 13: Reduction in feature size after transfer from polishing paper to PDMS 13
Figure 14: Optical images of (a) the sun facing side of a rose petal and (b) the post-imprinted rose petal PDMS sheet 14
Figure 15: Light scan analysis through air and through PDMS 15
Figure 16: MATLAB image analysis of light going through (a) air and (b) textured PDMS sheet 16
Figure 17: I-V curve comparing device performance with (red) and without (black) a textured sheet 17
Figure 18: Curled thin film product from the petri dish evaporation testing at a (a) top-down view and (b) side view 18
Figure 19: Dried sol-gel on a PDMS sheet after aging for 72 hours from a (a) top-down view and (b) side view 19
Figure 20: Crystallized final product of sol-gel cured on a hot plate 19
Figure 21: Post cured sol-gel applied via drop coating on a silicon wafer 20
Figure 22: Post cured single and triple layer sol-gel applied via spin coating on a Si wafer 21
Figure 23: Rapid heating method of (a) the solution after one hour, (b) the dried product on the sides of the beaker after ten hours, and (c) the remaining crystallized final product after ten hours 21

Chapter 1. Introduction

The desire for efficient clean energy has led to great strides in solar cell research in recent years. Via the photovoltaic effect, solar cells convert light energy into electricity and can reach open-circuit voltages of up to 0.5 to 0.6 V in single junction silicon devices [Green]. Silicon (Si) has long dominated the photovoltaics industry because of its low-cost, moderate efficiency, and ability to be manufactured on large scales. Si is also attractive because of its ability to be chemically etched along its crystallographic planes to form pyramidal shapes that scatter light and improve photon absorption in the device. Adding this antireflective coating (ARC) is a standard method to increase solar cell efficiency.

The photovoltaic community now also works with III-V type semiconductors grown epitaxially on a silicon substrate to increase efficiency above 30%. The Electronic Materials and Devices Laboratory has been working on a dual-junction cell with III-V grown epitaxially on a silicon bottom cell. However, the challenge that arises with using III-V materials is that it cannot be classically etched like silicon, so a new method had to be investigated to get the same light scattering effect through different means.

1.1 Antireflective coatings and textures

The absorption of light into a device generates an electron-hole pair that allows for charge carrier collection. This process can be improved by adding an ARC which would scatter the light, increase charge carrier path length, and ultimately increase device efficiency.

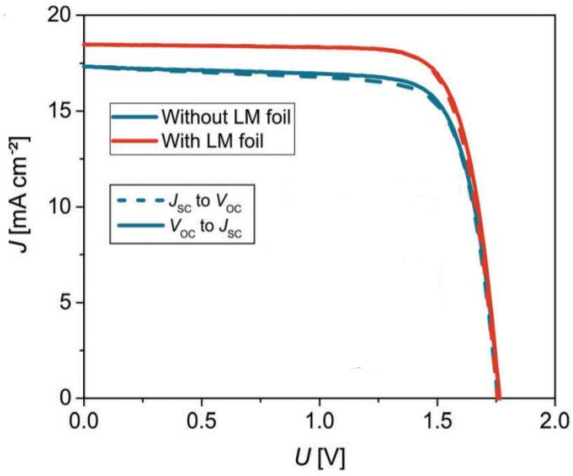

Figure 1: Increase in current density with addition of an antireflective coating [Marko]

Previous research has investigated alternate materials that could be patterned to act as an antireflective layer on solar devices. Figure 1 shows how the addition of a light management foil, a thin film textured glass-like structure, improved device efficiency by increasing short circuit current.

1.1.1 Pyramidal texture

In silicon, the most common method for path length enhancement is chemical etching which works by creating a surface of micro pyramids that disrupt the path of light into the device and decrease its entrance angle to increase the length it travels through the device [Marco]. Antireflective coatings are used in solar devices to scatter light which leads to charge carrier path length enhancement and increased absorption.

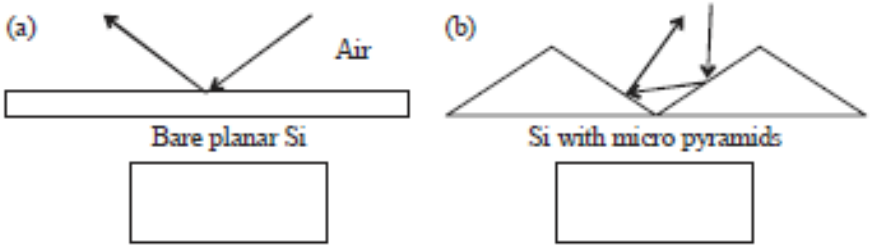

Figure 2: Reflection of incident light from (a) Bare planar Si and (b) Si micro pyramid texture [Al-Husseini]

1.1.2 Random texture

While pyramidal textures have been investigated extensively due to the popularity of Si based devices, there are other textures of interest. Random patterning could be used to scatter light, dependent on feature height and density. Having a mix of features could aid

in light scattering because varying feature angle promotes diverse light scattering and capturing light from more entrance positions [Forniés].

1.1.3 Biomimetic texture

Many biomimetic materials, like rose petals, have been investigated for their optical properties due to their superhydrophobicity and high contact angle being attractive features for light scattering behavior. This is expected for plant material because their survival and growth are dependent on their ability to absorb light, a characteristic also sought out in the photovoltaic community. Plant surfaces use their epidermal cell structure to reduce light loss due to reflectance by redirecting incoming photons, this causes a light focusing effect in devices which could increase efficiency [Hunig]. Biomimetic materials were also investigated in this work because they have properties that are attractive for photovoltaic applications because it should reduce optical loss that can occur in thin-film devices.

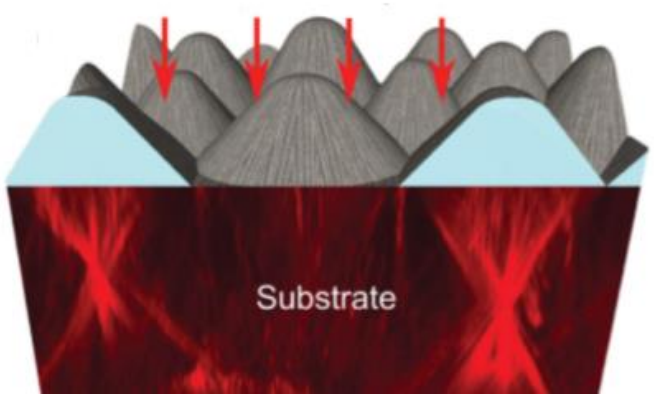

Figure 3: Cross section representation of a replicated rose structure coating on a substrate showing the light focusing effect. Adapted from [Hunig]

1.2 Polydimethylsiloxane texturization

Polydimethylsiloxane (PDMS) is a material of interest for texture imprinting and nanoimprint lithography. PDMS is a low-cost option with high optical transparency and a low refractive index of 1.4 which makes it an attractive option for an ARC. Figure 4 shows how the addition of a textured PDMS sheet decreases light reflection.

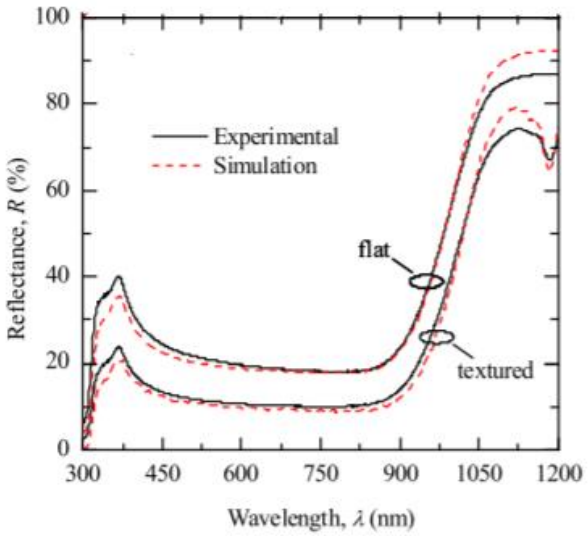

Figure 4: Simulated reflectance for 40 µm Si substrate with a 4 µm thick textured PDMS film on top. Adapted from [Rosell]

Related research has tested various patterns transferred to a PDMS sheet and positively changing the absorption profile of solar cells to increase efficiency. Current fabrication processes are not suitable to be scaled-up for largescale production and only temporary uses have been examined. PDMS is a temporary antireflective solution because over time it discolors and loses the integrity of the imprinted pattern. A more durable material must be utilized for a permanent solar cell top layer.

1.3 Sol-gel

Sol-gel is a low-cost process that involves a metal alkoxide precursor, a solvent and a catalyzing agent. It is an attractive method to produce protective coatings, fibers, powders, and thin films because of the wide array of parameters that give flexibility to the final product. The sol-gel process begins with a precursor and undergoes hydrolysis, condensation, gel formation, and drying until achieving the final product [Danks]. Sol-gel based films are attractive for optical films because the colloidal particles are on the order of nanometers and particle size can be controlled even more via precursor processing parameters. Reaction conditions are mild and the final product composition and structure can be easily controlled [Kócs].

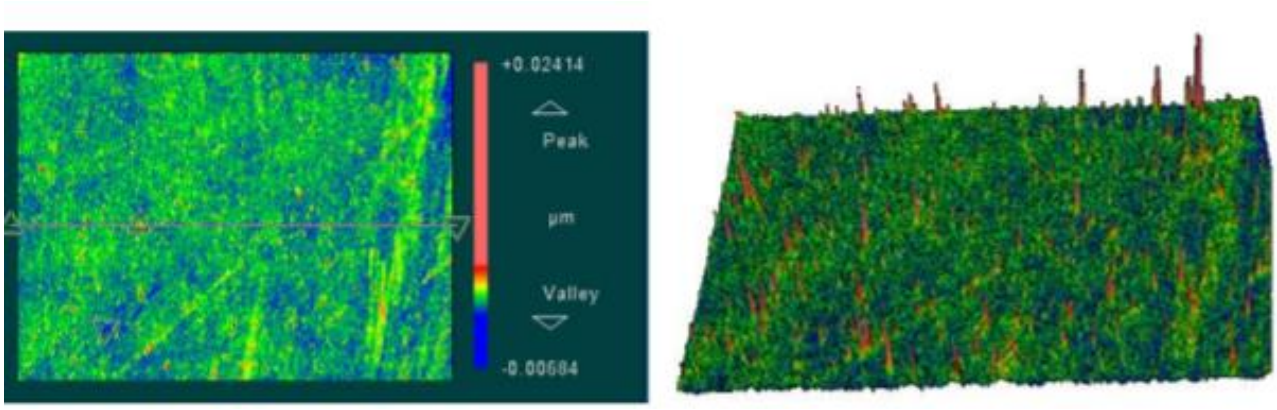

Figure 5: White-light interferometry measurement to of SiO_2 layer surface to determine area roughness [Thor]

Silica sol-gel processing involves the condensation and hydrolysis of tetraethyl orthosilicate that results in the suspension of colloidal oxide particles that form into the final oxide film. Silica has good thermal resistance, and the high transmission and selectivity that make it a good choice for a solar cell ARC [Dey].
An example of a resulting SiO_2 layer that forms from sol-gel processing can be seen in Figure 5. Silica sol-gel films often results in a very smooth surface with low area roughness parameters [Thor]. A smooth application is important for this experiment because the film will be imprinted with different textures to determine their effect on device efficiency so initial uniformity is key in processing.
Lastly, sol-gel can be applied using drop coating to accommodate complex shapes, which can be difficult for vapor deposition methods [Kumar]. Sol-gel allows for broad range of control in intermediate processing steps to have diversity in final products for its intended use.

1.4 Objective Statement

The purpose of this experiment is to determine the ability of PDMS to accept various textures and determine the optimal topographic features of those textures for an antireflective coating on a solar cell. The ARC is to be designed for materials that cannot be classically etched like Si, but can get the same benefits of increased absorption via path length enhancement caused by light scattering through a textured film. Since PDMS is not a permanent solution for a device ARC, the second part of this experiment will be investigating sol-gel as a thin film on a solar device that could be textured and serve as a permanent ARC.

Chapter 2. Methodology

2.1 Textured polydimethylsiloxane fabrication

The PDMS was synthesized with a 10:1 weight ratio of the Sylgard Silicon Elastomer 184 and Curing Agent 184, respectively. The mixture was stirred with a glass rod for five minutes to evenly distribute the curing agent. Due to the addition of gas into the solution after stirring, the mixture was held under a mild vacuum (<100 Torr) for 15 minutes to remove any bubbles that were introduced.

Multiple different materials were used to transfer surface features onto the PDMS and make textured sheets including various sized polishing paper (grit sizes 3, 6, and 9 µm) and biomaterials (flower petals).

To make the PDMS textured sheets with polishing paper, the papers were cut into 3 inch diameter circles and placed on a 0.5 inch thick piece of borosilicate glass. The glass was placed on a hot plate set to 50°C and a silo mold with 3 inch diameter was placed over the polishing paper and the uncured PDMS solution was filled in the mold to approximately 2 mm thick.

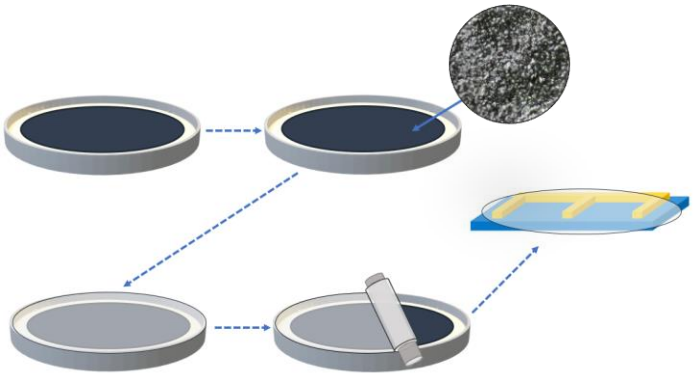

Figure 6: Textured PDMS sheet process schematic

This was cured for 5 hours on the hot plate and then allowed to cool for 12 hours prior to removal, as seen in Figure 6. The removal process had to be done using a glass rod (1 cm in diameter) in order to prevent the PDMS from ripping when being removed from the

texture material. Ripping was seen when an uneven amount of force was applied when manually removing the sheet. The glass rod was laid toward one end of the post-cured sheet and the sheet was slowly wrapped around the rod as it was rolled. The sheet could then be unwound from the rod, carefully, to avoid tearing.
Optical microscope images were taken of all PDMS sheets after processing. Feature height data was collected for the PDMS sheets processed using the 3 and 9 um polishing paper.
The same process was used to make the biomimetic sheets, aside from an additional solvent removal technique. Textured sheets were made to model the texture of a rose petal. After the PDMS curing process, the remaining rose petal residue on the PDMS and was removed via sonication in methanol for five minutes.

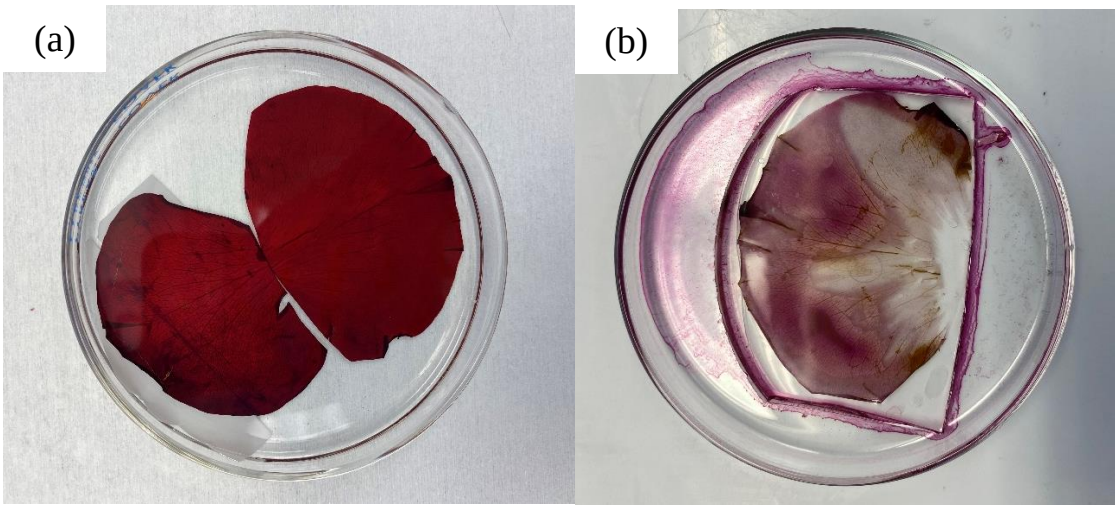

Figure 7: Processing of rose petal textured PDMS sheet (a) prior to petal removal and solvent sonification and (b) after solvent sonification and prior to final rinse

The last texture examined was pyramidal texture. The same fabrication process was used except the pattern was imprinted from a silicon solar cell that had been pyramidally etched using the standard alkaline {111} texturing process.

2.1.1 PDMS light scan testing

To test the efficacy of the pyramidally imprinted PDMS sheets, a 700 nm wavelength laser scan was used to evaluate light scattering. Figure 8 shows how a 5mW laser was shown at a detector covered by the PDMS. The detector was continuously shifted along the diameter of the textured sheet to map the light intensity getting through the sheet. The same process was performed for the laser through air. Values were recorded and plotted to determine light scattering caused by the textured PDMS sheet.

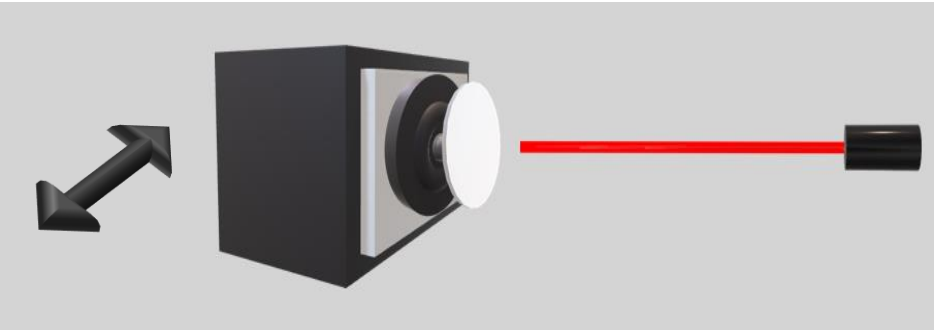

Figure 8: Light scan testing set-up

2.1.2 PDMS gray scale image testing

The next experiment performed was taking greyscale images of light going through air and through the sheets to quantify the light scattering through the sheet. The images were taken using a neutral density filter and a 10 ms exposure. Each pixel in the image corresponded to a relative intensity value. These images were analyzed via a MATLAB code that fit a line scan with a pseudo-Voigt model to calculate full width half max for both the light through air and light through PDMS tests.

2.1.3 PDMS solar simulating testing

A III-V dual junction device was tested in a solar simulator with 780 nm light on a 3.94 cm^2 surface area. The device was tested with and without the addition of a pyramidally textured sheet. For the test with the pyramidal textured sheet, water was used as a liquid filler suction method between the sheet and the device in an attempt to eliminate air gaps that may skew results.

2.2 Sol-gel synthesis and testing

The sol-gel solution was synthesized via an acid catalyzed reaction resulting in hydrolysis of tetraethyl orthosilicate (TEOS). One solution was made up of 24 mL of TEOS and 172 mL of ethanol and another solution was made of 1.6 mL of 2M HCl and 2.8 mL of H_2O. These two solutions were combined and magnetically stirred for one hour to achieve the final solution. The solution was then aged for five days prior to use. A sol-gel synthesis flow chart is provided in Figure 9.

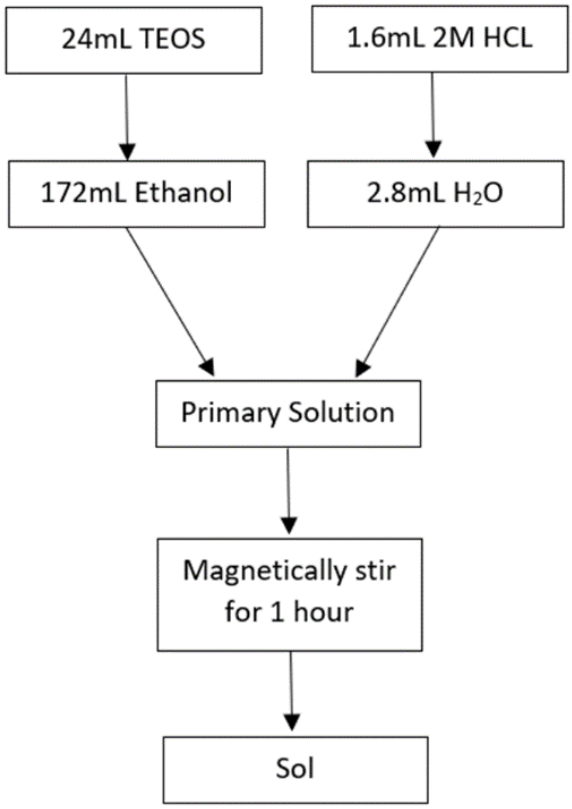

Figure 9: Flow chart of silica sol-gel processing

2.2.1 Sol-gel evaporation testing

Initial testing of the solution involved testing the effect of the sol in ambient conditions when left uncovered in a plastic dish. Two dishes were filled, one with 15 mL of solution and the other with 20 mL. All of these were aged in ambient conditions for 72 hours. This was done to analyze the amount of evaporation that would occur during aging of the solution.

A third evaporation test was a glass petri dish filled with 15 mL of the solution and cured uncovered on a hot plate at 500°C for 30 minutes.

2.2.2 Sol-gel thin film testing

Two different coating application methods were tested: drop coat and spin coat.

The sol was drop coated onto three substrates: 10 drops on a glass slide and 10 drops on a silicon wafer, and 25 mL over a textured PDMS sheet. All of these were covered with an airtight seal and then two tiny holes were created using pointed tweezers to allow for a small amount of air to be released to slow down the high rate of evaporation. The solvent

in the solution evaporates quickly and can result in film cracking. Because of this, slowing down the rate of volume loss by covering can prevent flaws.
These samples were cured in air for 72 hours. The silicon wafer was then heated in a furnace with a heating rate of 10°C per minute until 300°C, and then held for one hour and cooled back to room temperature in one hour.

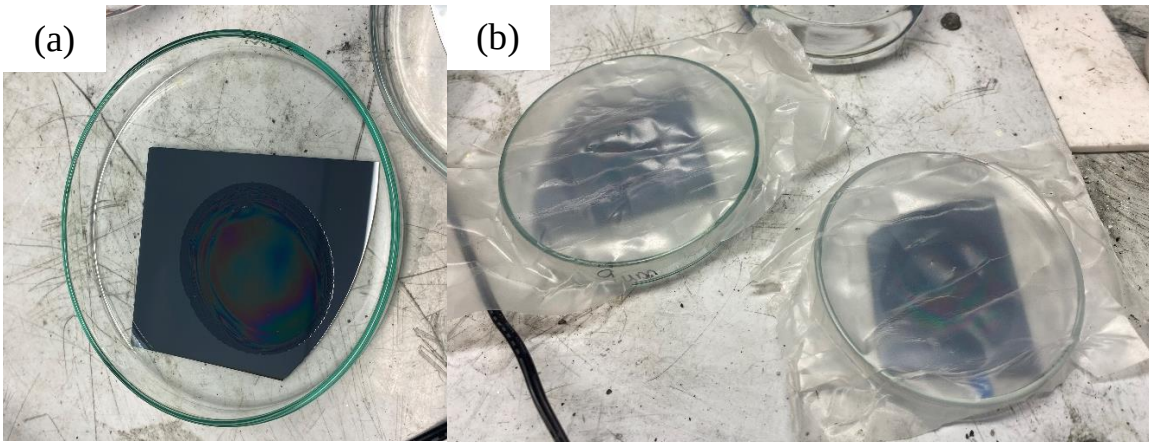

Figure 10: Drop coat (a) applied to a silicon wafer and (b) after being covered

Thin layers of the sol were also applied using a spin coater on two silicon wafers. One wafer had a single layer and the other had three layers. Each layer consisted of five drops being spun at a ramp up of 1200 rpm for 6 seconds then held at 3200 rpm for 30 seconds. The spin coater rpm values are based on values received by the spin coater used and are believed to have been slightly inaccurate. For the multi-layer wafer, the layers were allowed to age for 36 hours before another layer was added.
These were both cured in a furnace with a heating rate of 10°C per minute until 300°C, and then held for two hours and cooled back to room temperature in one hour. Optical images and layer thickness measurements were performed on the mono- and multi-layer spin coated samples.

2.2.3 Rapid evaporation

After processing the mono- and multi-layer spin coated samples for film thickness, it was determined that the film height was too small and would have to be increased to reap the optical benefits after imprinting texture. A rapid heating test was performed to determine how the viscosity of the solution would be changed as the solvent was evaporated from the sample.

An uncovered beaker containing 60 mL of the silica sol-gel solution was placed on a hot plate at 50°C under a fume hood. The solution was monitored every two hours for changes in volume and viscosity.

Chapter 3: PDMS Texturization

Texture was imprinted onto PDMS from three different sources: random texture from polishing paper, biomimetic texture from a rose petal, and pyramidal texture from an etched silicon wafer.

3.1 Random Texturization

Texture was retrieved from polishing paper of grits 3, 6, and 9 µm. The surface features were the most dense with the 9 µm polishing paper, as seen in Figure 11, which is the most beneficial for antireflective purposes.

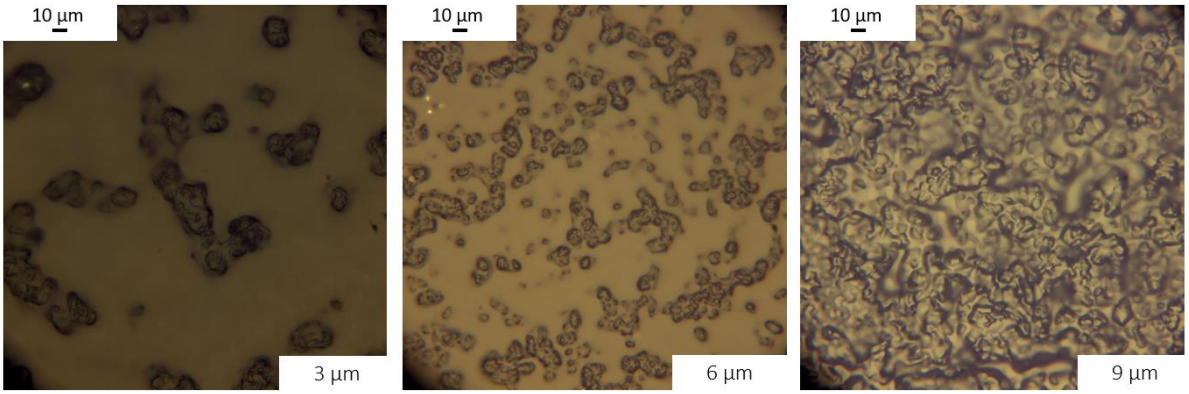

Figure 11: 50x magnification image of PDMS textured with polishing paper

The PDMS successfully transferred the texture from the paper onto the sample surface. Figure 12 shows the comparison of the textured PDMS to the corresponding 6 µm polishing paper that imprinted the PDMS. A temporary concern had been whether the textured PDMS matched its parent polishing paper because, when it was peeled off of the paper post-processing, it may have removed the surface features from the paper. It was confirmed using microscope analysis that the texture was imprinted into the PDMS so that when used as a stamp it could produce extruded surface features.

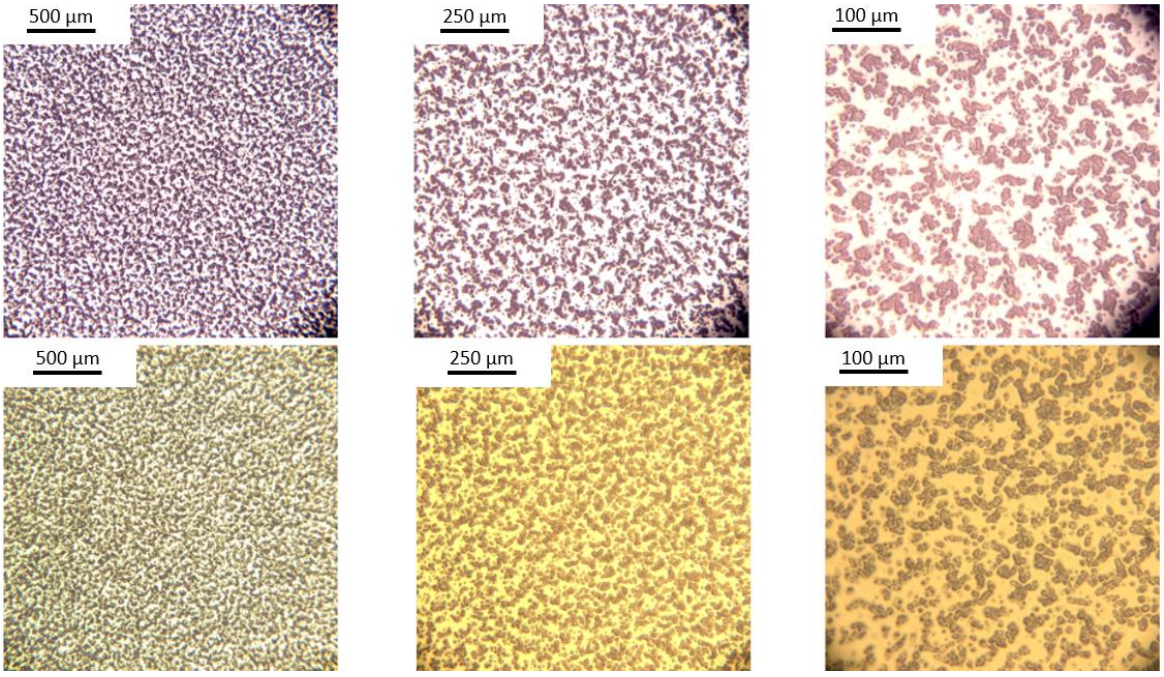

Figure 12: 6 µm polishing paper (top) and PDMS textured with the 6 µm paper (bottom)

3.1.1 Profilometry

While we can see that the general features were transferred well from the paper to the sheet, feature height measurements were taken from the 3 and 9 µm textured PDMS sheets using a profilometer. There was a 23.2% and 34.4% reduction in feature height in the 3 and 9 µm textured sheets, respectively. This height change can be seen in Figure 13.

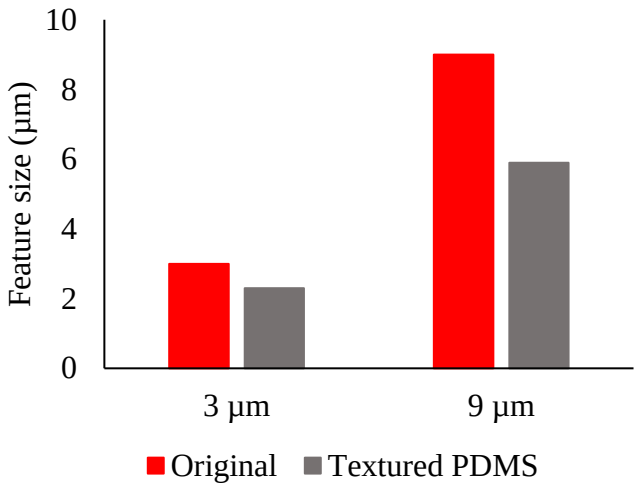

Figure 13: Reduction in feature size after transfer from polishing paper to PDMS

3.2 Biomimetic

Texture was transferred from the sun-facing side of a rose petal to a PDMS sheet. Figure 14 shows the comparison between a microscopic image taken of a rose petal surface facing the sun and the PDMS with the petal imprint. This confirms that the petal features were successfully transferred onto the PDMS sheet with an indented papillae structure. The papillae features give roses their high-adhesive superhydrophobic properties which is desirable for optical applications.

These images also confirm successful transfer of the petal features to the PDMS with limited residual biomaterial stuck to the sheet's surface. Residual material left on an antireflective coating surface would be costly to its performance because light blocking would decrease device absorption.

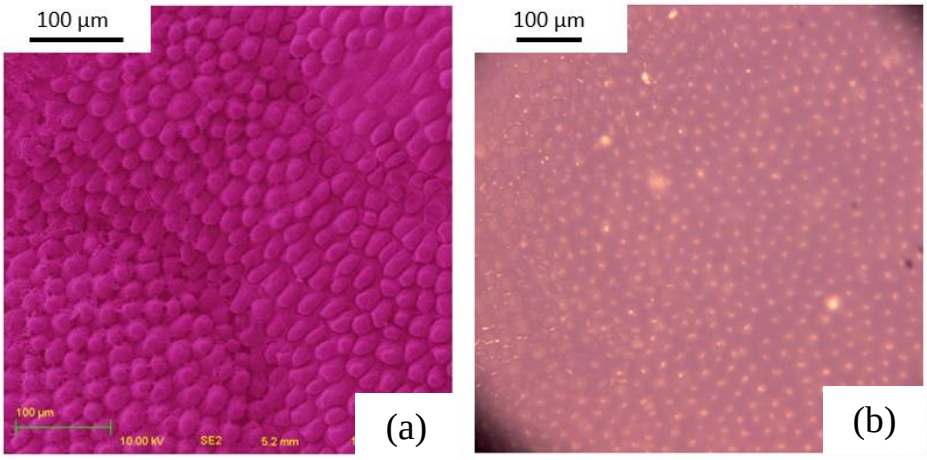

Figure 14: Optical images of (a) the sun facing side of a rose petal and (b) the post-imprinted rose petal PDMS sheet

Chapter 4: PDMS Optical Characterization and Testing

4.1 Light scan analysis

A laser scan performed on the PDMS sheet confirmed an increase in peak width compared to the laser through air, shown in Figure 15.

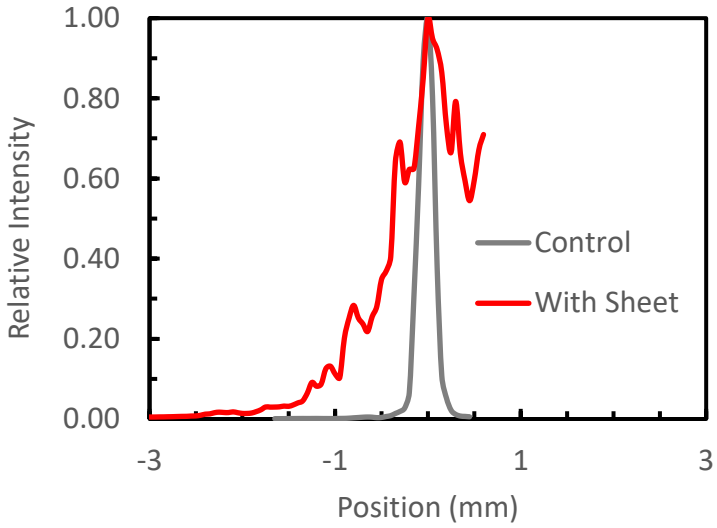

Figure 15: Light scan analysis through air and through PDMS

4.2 Grayscale image light scatter testing

Grayscale images were captured using a charged couple device (CCD). One image was taken through just air and one through the pyramidally textured PDMS sheet. The images were processed as a collection of pixels where each is stored as an 8-bit integer with a value from 0 to 255, where 0 is black and 255 is white.

A 10-pixel width line scan was taken through the peak of both of the images and averaged to calculate and compare the light scattering. Both scans were fitted with a pseudo-Voigt model. The full width half max (FWHM) values were determined to be 136.2 and 237.2 pixel distances from peak for the control plot and the with sheet plot, respectively. Overall, there was a 74.2% increase in FWHM with addition of the textured sheet.

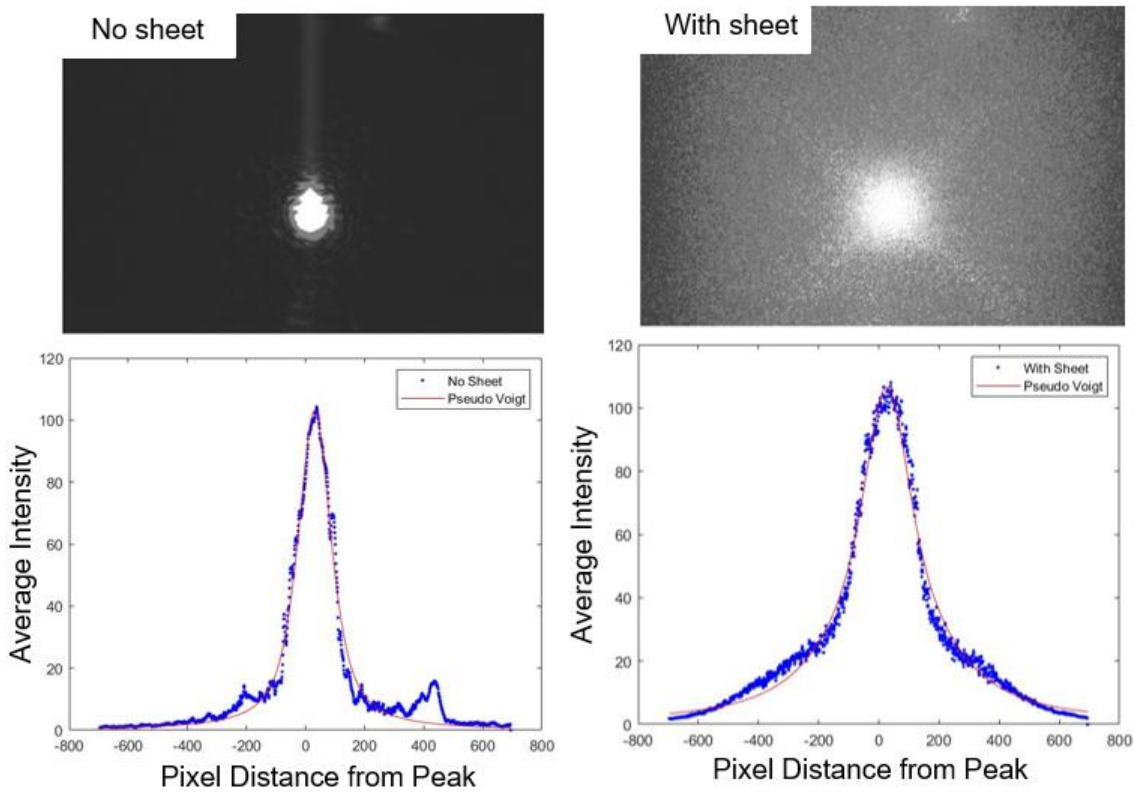

Figure 16: MATLAB image analysis of light going through (a) air and (b) textured PDMS sheet

4.3 Solar Simulator Analysis

Final testing performed on the pyramidal textured sheet was done to determine its overall effect on device efficiency. The sheet was used on a III-V dual junction solar cell with an area of 3.94 cm^2 and tested under a 780 nm wavelength light. Figure 17 shows the results of the solar simulator test comparing the device performance with and without the addition of the textured PDMS sheet.

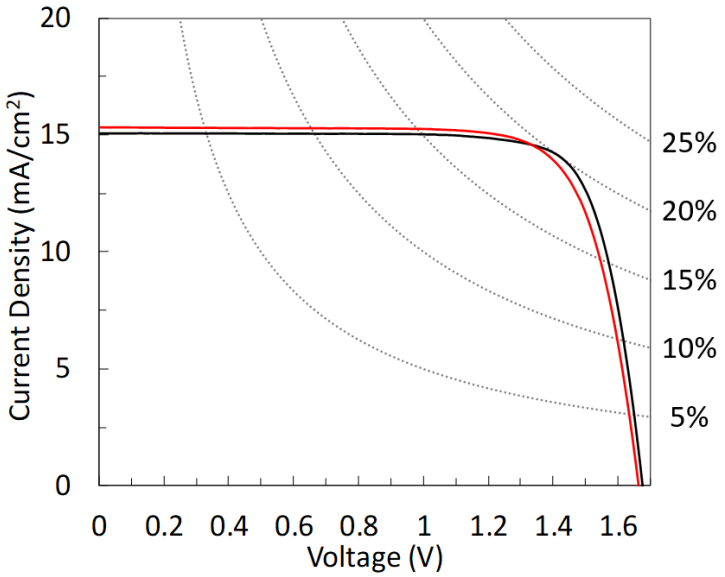

Figure 17: I-V curve comparing device performance with (red) and without (black) a textured sheet

Short circuit current density value increased from 15.06 to 15.34 mA/cm^2 with addition of the textured sheet. However, there was a drop in fill factor concurrent with the increase in short circuit current due to a decrease in open circuit voltage from 1.59 to 1.54 V. This resulted in a fill factor drop from 85.9% to 83.6% with the addition of the sheet and ultimately corresponded with a decrease in device efficiency. A possible explanation for this behavior is because water was used to adhere the sheet to the device surface which may have interfered with carrier behavior by decreasing its absorption by causing additional and unwanted reflectance. This adherence method was also tested with isopropyl alcohol and resulted in the same effect.

Chapter 5: Sol Gel Fabrication and Analysis

5.1 Sol gel evaporation testing

After processing the initial sol-gel solution, it was tested without being applied to a substrate to determine how it behaves when it evaporates at different conditions. 15 mL and 20 mL of solution were deposited in two petri dishes and allowed to age uncovered in ambient conditions. Figure 18 shows the resulting curled thin film product that was observed for both the 15 mL and 20 mL dishes. This behavior was likely due to the rapid evaporation since the dish was uncovered and the quick volume loss caused the film to crack, shrink and curl at the ends.

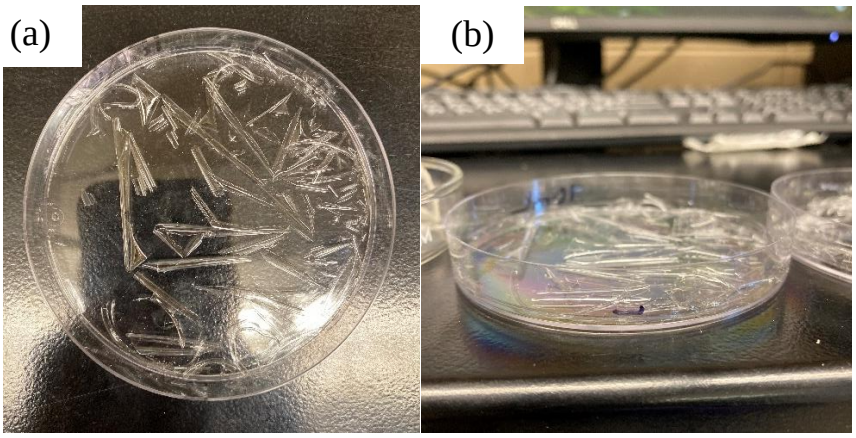

Figure 18: Curled thin film product from the petri dish evaporation testing at a (a) top-down view and (b) side view

15 mL of the solution was also tested on a PDMS sheet and aged in ambient conditions for 72 hours. As seen in Figure 19, the same behavior was observed as what was seen in the dishes without substrates. The solution coated the PDMS and, as the solvent evaporated quickly, it caused the PDMS to shrink and curl. There is also cracking present due to the rapid loss in volume.

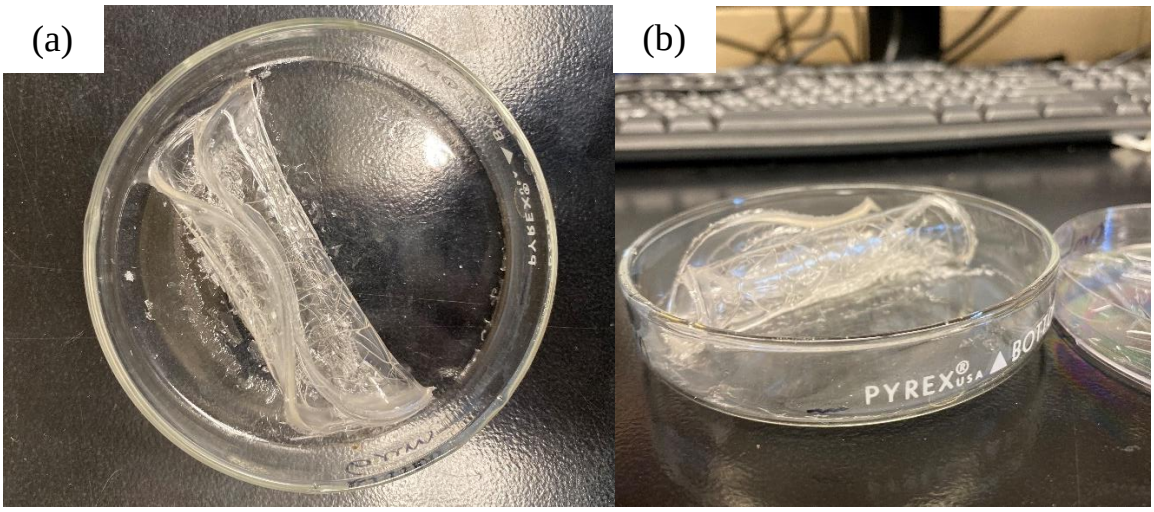

Figure 19: Dried sol-gel on a PDMS sheet after aging for 72 hours from a (a) top-down view and (b) side view

Lastly, 15 mL of solution was added to a glass petri dish and cured uncovered on a hot plate at 500°C for 30 minutes. This was done in accordance with the literature for an appropriate full curing of the solution into a hard film. The resulting product, seen in Figure 20, was a collection of crystallized SiO_2 chunks. The solution began to bubble immediately as it was heated and was evaporated too quickly to form an even film.

Figure 20: Crystallized final product of sol-gel cured on a hot plate

5.2 Sol-gel wafer drop coat application

The drop coat and spin coat methods were used to apply the sol solution onto varying surfaces. In both cases, it resulted in a crystallized thin film.

For the drop coat method, two wafers were tested, one with and one without PDMS texture imprinting. Optical microscope images, seen in Figure 21, confirm that texture did transfer from the PDMS to the final sol-gel film but further testing did not confirm the extent or accuracy of much the film was imprinted.

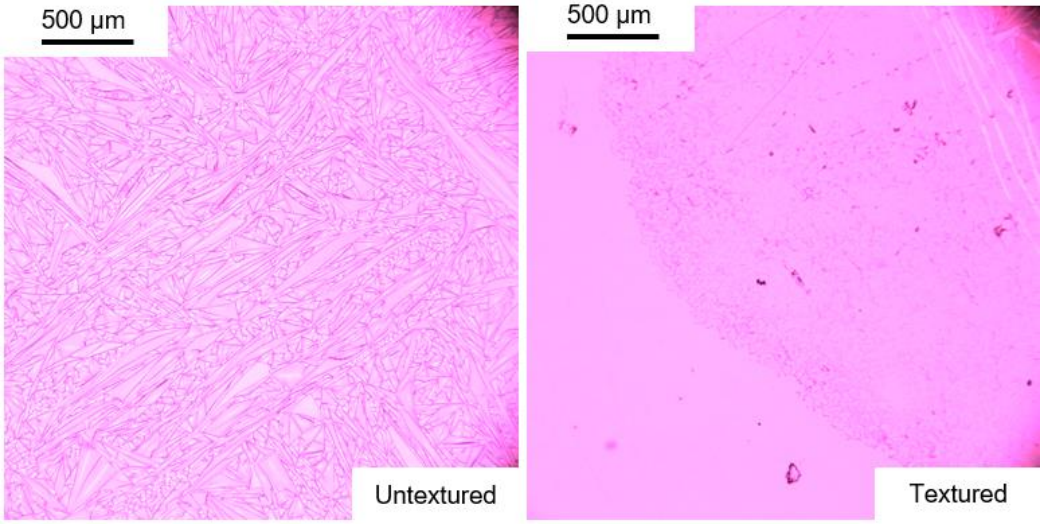

Figure 21: Post cured sol-gel applied via drop coating on a silicon wafer

5.3 Sol gel wafer spin coat application

Spin coating was the second application method tested and was applied on a silicon wafer in a single and triple layer. Figure 22 shows how spin coating caused an unwanted directionality in the film. The triple layer also seemed to have small particles that hindered solution uniformly spreading on the surface. These may have been a result of colloidal particles forming after being applied, or outside dust that landed on the wafer between layers.

Thickness measurements were taken on both wafers and had film heights of 130 nm and 350 nm for the single and triple layered samples, respectively. Since optimal feature height for its intended ARC purpose is approximately 5-10 µm, this method is not a viable option for future textured films unless there was an increase in solution viscosity prior to application that resulted in increased film thickness.

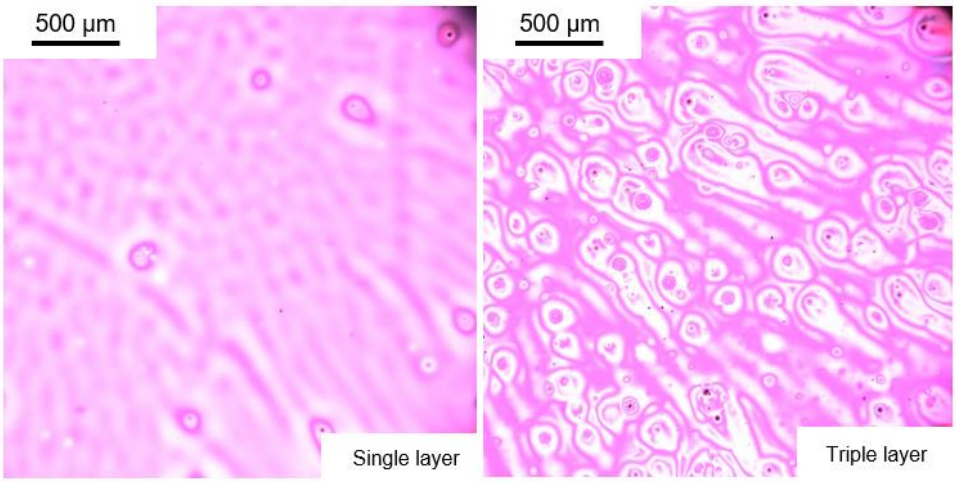

Figure 22: Post cured single and triple layer sol-gel applied via spin coating on a Si wafer

5.4 Sol gel rapid heating

Due to the film thicknesses being too small for adequate texture transfer from any of the textured PDMS sheets, it was determined that viscosity of the solution would have to be increased prior to application (via drop or spin coating) in order to produce a thicker film. A rapid heating method was attempted using 60 mL of solution heated at 50°C and monitored closely for an increase in viscosity. This was done in an attempt to decrease solvent volume and thicken the overall solution. At ten hours, the solution was completely evaporated and only crystallized chunks of primarily SiO_2 remained.

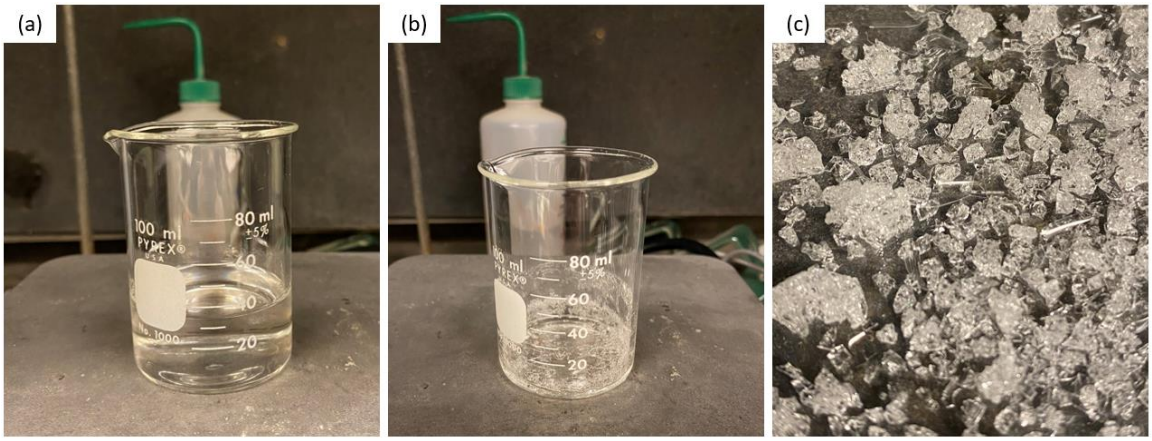

Figure 23: Rapid heating method of (a) the solution after one hour, (b) the dried product on the sides of the beaker after ten hours, and (c) the remaining crystallized final product after ten hours

There was little to no change in viscosity during this test. The primary outcome was complete evaporation and an impossibly narrow window in which the solution went from very fluid to completely crystalized. It is assumed that the colloidal particles in the solution grow as the solvent evaporates as the solution mixes and reacts with oxygen in the air. This method was not a viable technique to increase viscosity of the sol-gel. An increase in the volume of solution tested may be beneficial for future experiments because a more long-term view of the viscosity could be observed. Also, the solution could be covered or held in a controlled atmosphere to limit the amount of oxygen able to react with the solution.

Chapter 6: Conclusion

6.1 PDMS

6.1.1 PDMS texturization

The random, biomimetic, and pyramidal textures were successfully transferred to the PDMS sheets using a simple and low-cost process. The loss in feature height may have been due to circumstances prior to processing, such as damage during transport.

6.1.2 PDMS optical analysis

MATLAB line scan analysis of light through air compared to light scattered through a pyramidally textured sheet resulted in a 74.2% increase in the full width half max when plotted using a pseudo-Voigt model. Further analysis using images captured through a CCD camera should work to remove the oversaturation observed in the images that may skew scattering data.

The pyramidally textured sheet also resulted in an increase in the short circuit current. However, a drop in open circuit voltage was also observed so the sheet did not result in an overall increase in device efficiency. It is speculated that the drop in open current voltage may have resulted due to the adherent method obstructing electrical efficiency. Future testing could employ an index matching fluid to suction the sheet.

6.2 Sol gel

The sol-gel method, while simple in processing, is not a viable option for a permanent textured top layer due to film thicknesses that resulted from the application techniques used in this research. The silica colloidal particles that formed in the solution, while smaller than optimum texture feature size, may decrease optical properties and make a sol-gel based ARC less effective. Further testing could be done to increase solution viscosity prior to application to result in an increased film thickness.

6.3 Future work

More research should be done to test a variety of patterns to determine their effect on device efficiency. Biomimetic materials exhibiting superhydrophobic properties are of interest but more imaging should be done on post processed biomimetic textured sheets to determine if all feature aspects of the superhydrophobic papillae were imprinted. Further testing should be performed on all the textured sheets fabricated during this research to determine the efficacy of the patterning and its effect on reflectivity.

The MATLAB analysis can be used to provide additional investigation into the differences between the varying textures and do ray tracing to map how the light is traveling through the textured sheets.

Alternate materials to serve as a permanent top coating should also be examined. Melting gels are an attractive option for this application due to their ability to be liquid at high temperatures until a certain cross-linking temperature at which point the solution forms additional bonds and becomes a solid when returned to room temperature.

Bibliography

Al-Hussseini, A., & Lahlouh, B. (2017). Silicon Pyramid Structure as a Reflectivity Reduction Mechanism. Journal of Applied Sciences. 17(8), 374-383

Danks, A., Hall, S., and Schnepp, Z. (2016). The evolution of 'sol-gel' chemistry as a technique for materials synthesis. Mater. Horiz. 3, 91-112. doi:10.1039/C5MH00260E

Dey, T., & Naughton, D. (2019). Nano-porous sol-gel derived hydrophobic glass coating for increased light transmittance through greenhouse. *Materials Research Bulletin,* 116, 126-130. doi:10.1016/j.materresbull.2019.04.027

Forniés, E., Zaldo, C., & Albella, J.M. (2005). Control of random texture of monocrystalline silicon cells by angle-resolved optical reflectance. *Solar Energy Materials and Solar Cells*, 87(1-4), 583-593. doi: 10.1016/j.solmat.2004.07.040

Green, M. A. (2009). Progress in Photovoltaics: Research and Applications. *Prog. Photovolt: Res. Appl, 17*, 183-189. DOI: 10.1002/pip.892

Hunig, R. (2016). Flower Power: Exploiting Plants' Epidermal Structures for Enhanced Light Harvesting in Thin-Film Solar Cells. Advanced Optical Materials, 4, pp. 1487-1493

Kócs, L., Albert, E., Tegze, B., Kabai-Faix, M., Major, C., Szalai, A., Basa, P. and Hórvölgyi, Z. (2018) Silica Sol-gel Coatings with Improved Light Transmittance and Stability. *Periodica Polytechnica Chemical Engineering*, 62(1), 21-31. doi: 10.3311/PPch.10550.

Kumar, Amit & Singh, Rajeev & Bahuguna, Gaurav. (2016). Thin Film Coating through Sol-Gel Technique. Research Journal of Chemical Sciences. 6. 65.

Marko, J. (2018). Textured interfaces in monolithic perovskite/silicon tandem solar cells: advanced light management for improved efficiency and energy yield. *Energy & Environmental Science, 11,* 12, 3511-3523

Notten, P.H.L. (1989). Electrochemical study of the etching of III-V semiconductors. Eindhoven: Technische Universiteit Eindhoven. https://doi.org/10.6100/IR307988

Rosell, A., Martin, I., Garin, M., Lopez, G. & Alcubilla, R. (2020). Textured PDMS Films Applied to Thin Crystalline Silicon Solar Cells. IEEE Journal of Photovoltaics. 10(2), 351-357

Schmager, R., Fritz, B., Hunig, R., Ding, K., Lemmer, Uli., Richards, B., Gomard, G., & Paetzold, U. (2017). Texturization of the Viola Flower for Light Harvesting in Photovoltaics. ACS Photonics, 4, 2687-2692. pubs.acs.org.

Thor, T., & Vaclavik, J. (2016). Sol-gel preparation of Silica and Titania thin films. Paper presented at the Optics and Measurement International Conference, Liberec, CZECH REPUBLIC.

Torum, I., Celik, N., Hancer, M., et al. (2018). Water Impact Resistance and Antireflective Superhydrophobic Surfaces Fabricated by Spray Coating of Nanoparticles: Interface Engineering via End-Grafted Polymers. Macromolecules 51(23), 10011-10020. doi: 10.1021/acs.macromol.8b01808

Womack, G., Isbilir, K., Lisco, F., Durand, G., Taylor, A., Walls, J. (2019) The performance and durability of single-layer sol-gel anti-reflection coatings applied to solar module cover glass. Surface and Coatings Technology, 358, pp. 76-83.